Gravitational waves from thermal heavy scalar dark matter

Parsa Ghorbani
Physics Department, Faculty of Science, Ferdowsi University of Mashhad, Iran

(Received 30 August 2024; accepted 14 November 2024; published 3 December 2024)

We propose a gauge singlet scalar with mass around 1–100 TeV as a thermal heavy dark matter candidate along with a dilaton as a Higgs portal mediator in a dimensionless scalar extension of the Standard Model. We demonstrate analytically that such a model gives rise to very strong first-order electroweak phase transition through supercooling. We calculate the corresponding gravitational wave signals due to bubble collisions during the phase transition. The produced gravitational waves can be detected by future space-based gravitational wave detectors in the frequency range from 10^{-4} to 0.1 Hz.

DOI: 10.1103/PhysRevD.110.115002

I. INTRODUCTION

After the discovery of first spin zero scalar elementary particle at the LHC in 2012 [1–3], it has been a reasonable assumption to expect more scalars in nature. While the existence of other types of particles is possible in beyond the standard model (BSM), but an addition of even one scalar degree of freedom apart from the Higgs particle, complicates significantly the process of the electroweak symmetry breaking [4,5]. The scalar extensions of the standard model have been always of interest to explain the theoretical and observational shortcomings of the stand ard model (SM). Additional scalars may accommodate the dark matter problem [6–10], or to impose the electroweak symmetry breaking in the early universe be strongly first order for a successful explanation of the observed matter-anti matter asymmetry in the universe [11], through which gravitational wave signals can be detected [12,13], or to address a combination of the aforementioned problems [14–16].

Additional scalars can be employed in dimensionless extensions of the SM to address additionally the hierarchy and fine-tuning problems. There are scale invariant models that have tried to explain one or more problems such as dark matter or electroweak phase transition [17–24]. Although it is known that electroweak phase transition in scale invariant scalar extension of the SM is very strong [19], but the possibility of detecting the gravitational waves signals produced during such phase transitions when an extra scalar plays the role of a thermal heavy dark matter has not been investigated in the literature. A nonthermal heavy dark matter scenario from first-order phase transition is studied in [25].

The main points we will highlight in this work before going into the details are as follows:

(i) The model lies within the Gildener-Weinberg scale invariant approach, therefore the electroweak phase transition occurs only via Coleman-Weinberg radiative corrections.
(ii) After the symmetry breaking, there is always a heavy scalar which is stable and can be dark matter candidate.
(iii) Even with very small couplings, the heavy dark matter can be produced thermally in early universe.
(iv) The electroweak phase transition is first-order and very strong. We show this analytically in high temperature approximation.
(v) The dominant contribution in producing the gravitational waves is due to the bubble wall collisions.
(vi) The gravitational waves produced by EWPT is detectable only in future GW detectors.

The paper is organized in the following order. In Sec. II, we introduce the dimensionless extension of the SM, and define the free parameters and will give the effective potential after the EWSB. In Sec. III, we show how the EWPT in this model is strongly first-order. In Sec. IV, we introduce the heavy dark matter candidate and calculate its relic density. We also calculate the spin-independent DM-nucleon cross section and confront the result with the direct detection bounds. In Sec. V, we calculate possible gravitational wave signals when the parameter space is restricted already by heavy dark matter. We conclude with the results in Sec. VI.

II. MODEL

The model consists of a two gauge singlet scalars coupled to the Higgs within the scale invariant extension of the SM. Among two singlet scalars one gains mass via

radiative corrections and the other is heavy according to Gildener-Weinberg [26]. The heavier scalar is taken as the DM candidate while the lighter scalar, the so-called scalon field, is the SM-DM mediator. The bare potential with adimensional couplings consisting of the Higgs doublet and two singlet scalars before the electroweak symmetry breaking (EWSB) read

$$V(\phi_1,\phi_2,\phi_3)=\frac{1}{4}\lambda_1\phi_1^4+\frac{1}{4}\lambda_2\phi_2^4+\frac{1}{4}\lambda_3\phi_3^4+\frac{1}{2}\lambda_{12}\phi_1^2\phi_2^2+\frac{1}{2}\lambda_{13}\phi_1^2\phi_3^2+\frac{1}{2}\lambda_{23}\phi_2^2\phi_3^2 \tag{1}$$

where ϕ_1 is the neutral component of the Higgs doublet $H^\dagger=(0\,\phi_1)/\sqrt{2}$ in unitary gauge, and ϕ_2 and ϕ_3 are real singlet scalars.

The scale symmetry breaking which subsequently leads to electroweak symmetry breaking takes place through radiative corrections. According to Gildener-Weinberg approach there exists a flat direction in the field space along which the potential and its minimum is vanishing. In our model, the flat direction with three scalar field is three-dimensional (n_1,n_2,n_3). As the third scalar, i.e., ϕ_3 is the DM candidate here, it does not acquire a nonzero VEV, therefore we set $n_3=0$ and the flat direction will be in (ϕ_1,ϕ_2) space.

$$\phi_1=n_1\phi\equiv\phi\sin\theta,\qquad \phi_2=n_2\phi\equiv\phi\cos\theta, \tag{2}$$

where $n_1^2+n_2^2=1$ and $\phi^2=\phi_1^2+\phi_2^2$ is the radial field. The flat direction is given by

$$\sin^2\theta\equiv n_1^2=\frac{\lambda_{12}}{\lambda_{12}-\lambda_1},\qquad \cos^2\theta\equiv n_2^2=\frac{\lambda_1}{\lambda_1-\lambda_{12}}. \tag{3}$$

The Coleman-Weinberg one-loop effective potential along the flat direction is given by

$$V_{\rm eff}^{\rm 1-loop}(\phi)=B\phi^4\left(\log\frac{\phi}{\langle\phi\rangle}-\frac{1}{4}\right) \tag{4}$$

where $\langle\phi\rangle$ is the VEV of the radial field and B is a dimensionless coupling given in general by

$$B=\frac{1}{64\pi^2\langle\phi\rangle^4}(\mathrm{Tr}M_S^4+3\mathrm{Tr}M_V^4-4\mathrm{Tr}M_F^4) \tag{5}$$

in which M_S, M_V and M_F denote respectively the mass matrices for scalars, vectors and fermions in the model. In particular, for the model we are considering

$$B=\frac{1}{64\pi^2\langle\phi\rangle^4}(m_{\rm DM}^4+m_H^4+6m_W^4+3m_Z^4-12m_t^4) \tag{6}$$

where $m_{\rm DM}\equiv m_{\phi_3}$. The effective potential in Eq. (14), in addition to having a minimum at zero it develops a deeper minimum for a nonzero VEV, so that the symmetry is radiatively broken at one-loop level. Through the VEV of the radial field, $\langle\phi\rangle$, scalars ϕ_1 and ϕ_2 take nonzero VEVs. Subsequently, there is a mixing among scalars ϕ_1 and ϕ_2 and their mass matrix will not be diagonalized. Rotating the (ϕ_1,ϕ_2) into a new basis (h,s) defined as

$$\begin{pmatrix}h\\ s\end{pmatrix}=\begin{pmatrix}\cos\theta & \sin\theta\\ -\sin\theta & \cos\theta\end{pmatrix}\begin{pmatrix}\phi_1\\ \phi_2\end{pmatrix} \tag{7}$$

will diagonalize the mass matrix with mass eigenvalues

$$m_H^2=-2\lambda_{12}\langle\phi\rangle^2, \tag{8a}$$

$$m_{\rm DM}^2=(\lambda_{13}\sin^2\theta+\lambda_{23}\cos^2\theta)\langle\phi\rangle^2, \tag{8b}$$

$$m_s=0. \tag{8c}$$

As anticipated in GW approach one of the scalars (here scalar s) is massless which is known as *scalon*. The dynamical symmetry breaking gives a small mass to the classically massless scalon s

$$\delta m_{\rm s}^2=8B\langle\phi\rangle^2=\frac{1}{8\pi^2\langle\phi\rangle^2}\times(m_H^4+6m_W^4+3m_Z^4-12m_t^4+m_{\rm DM}^4). \tag{9}$$

Considering the latest experimental values for heavy SM particle masses being $m_H=125.12$ GeV, $m_Z=91.19$ GeV, $m_W=80.38$ GeV, $m_t=172.76$ GeV, and the fact that the scalon mass must be positive, i.e., $\delta m_{\rm s}^2>0$, the DM mass is bounded from below: $m_{\rm DM}>316.12$ GeV. In order to get small scalon mass, its VEV must be considerably large; for instance if $v_s=1000$ GeV then $m_{\rm s}\simeq 10$ GeV. The effective potential after the electroweak symmetry breaking read

$$\begin{aligned}V_{\rm tr}(h,s,\phi_3)=&-\lambda_{12}[\langle\phi\rangle^2h^2+2\langle\phi\rangle h^3\cot(2\theta)+h^4\cot^2(2\theta)+h^2s^2+2\langle\phi\rangle h^2s+2h^3s\cot(2\theta)]\\&+\frac{1}{2}[\lambda_{13}\sin^2(\theta)+\lambda_{23}\cos^2(\theta)][s^2\phi_3^2+\langle\phi\rangle^2\phi_3^2+2\langle\phi\rangle s\phi_3^2]+\frac{1}{2}[\lambda_{13}\cos^2(\theta)+\lambda_{23}\sin^2(\theta)]h^2\phi_3^2\\&+\frac{1}{2}(\lambda_{13}-\lambda_{23})\langle\phi\rangle h\phi_3^2\sin(2\theta)+\frac{1}{4}\lambda_3\phi_3^4\end{aligned} \tag{10}$$

where θ is the mixing angle.

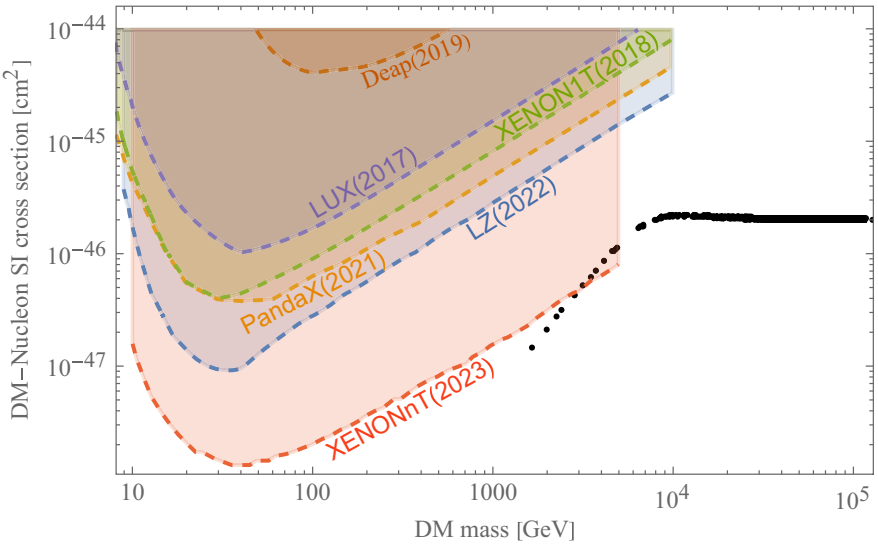

FIG. 1. The DM-nucleon cross section is shown. Almost all the parameter space for DM masses heavier than 1.5 TeV is evaded from direct detection constraints.

III. HEAVY SCALAR DARK MATTER

From the LHC Higgs phenomenology the mixing angle is constrained as $\cos\theta > 0.85$ or $-0.555 < \theta < 0.555$. The Higgs field VEV is fixed $v_h = 246$ GeV, and the singlet scalar VEV is determined through the scale symmetry breaking scale $\langle\phi\rangle$ by $\langle\phi\rangle^2 = v_h^2 + v_s^2$. Taking into account that $\tan\theta = v_h/v_s$ and choosing the scale $\langle\phi\rangle$ as a free parameter, the mixing angle is fixed by $\cot^2\theta = \langle\phi\rangle^2/v_h^2 - 1$. The larger the scale of $\langle\phi\rangle$, the smaller the mixing angle will be; the minimum value is $\langle\phi\rangle_{\rm min} \simeq 466$ GeV for $\theta \simeq 0.555$. The coupling λ_{12} is determined by $m_H^2 = -2\lambda_{12}\langle\phi\rangle^2$ with $m_H \simeq 125$ GeV. The coupling λ_1 is not free as it is fixed from Eq. (3). Similarly for the coupling λ_2 which is obtained from the flat direction condition $\lambda_2 = \lambda_{12}^2/\lambda_1$. Therefore, the space of free parameters is as restricted as $\{\langle\phi\rangle, \lambda_{13}, \lambda_{23}, \lambda_3\}$. As pointed out before the dark matter candidate is the field ϕ_3 with vanishing VEV which makes it a stable particle. Its relic density is obtained by the Boltzmann equation for thermal evolution of dark matter field number density $n_{\rm DM}$,

$$\frac{dn_{\rm DM}}{dt} + 3Hn_{\rm DM} = -\langle\sigma_{\rm ann} v_{\rm rel}\rangle[n_{\rm DM}^2 - n_{\rm DM}^{\rm eq\,2}] \quad (11)$$

in which $n_{\rm DM}^{\rm eq}$ stands for the DM number density in plasma thermal equilibrium in the early universe, H is the Hubble expansion rate, $v_{\rm rel}$ is the dark matter relative velocity and $\sigma_{\rm ann}$ is the dark matter annihilation cross section.

We have used the package MicrOMEGAs6.0 to numerically calculate the relic abundance of the heavy dark matter. The model accommodates the DM relic density $\Omega_{\rm DM}h^2 \simeq 0.12$ observed by WMAP and Planck [27,28]. The results in Fig. 2 show that respecting the observed relic density value, the lighter DM requires larger Higss portal coupling λ_{12}. Inversely, the larger DM mass requires larger coupling λ_{23}. The DM mass predicted in this model is above 1.5 TeV.

The parameter space in the model is strongly constrained by DM-nucleon cross section the direct detection experiments [29–35]. The effective DM-nucleon interaction Lagrangian is

$$\mathcal{L}_{\rm eff} = \alpha_q \phi_3 \phi_3 \bar{q} q \quad (12)$$

where α_q is the DM-quark coupling. This leads to spin-independent (SI) DM-nucleon scattering cross section

$$\sigma_{\rm SI}^{\rm N} = \frac{\alpha_N^2 \mu_N^2}{\pi m_{\rm DM}^2} \quad (13)$$

with μ_N being the reduced DM-Nucleon mass and α_N a coefficient depending on nucleon form factors [36]. We have used the MicrOMEGAs6.0 package to calculate the DM-nucleon scattering cross section. The result is shown in Fig. 1. Although the parameter space is already restricted from the DM relic abundance, we see in Fig. 1 that except from a small region of the parameter space, the model is evaded from the direct detection constraints.

IV. ELECTROWEAK PHASE TRANSITION

We assume that the scale symmetry is broken at high enough temperatures respect to the masses in the model so that we can use the high-temperature expansion.[1]

[1]If $m/T \lesssim 1.6$, the high-temperature approximation agrees better than 5% with the exact thermal potential. For large values of m/T, still the high-temperature approximation is valid up to 10% due to suppressed Boltzmann contribution (see Appendix B in [37]).

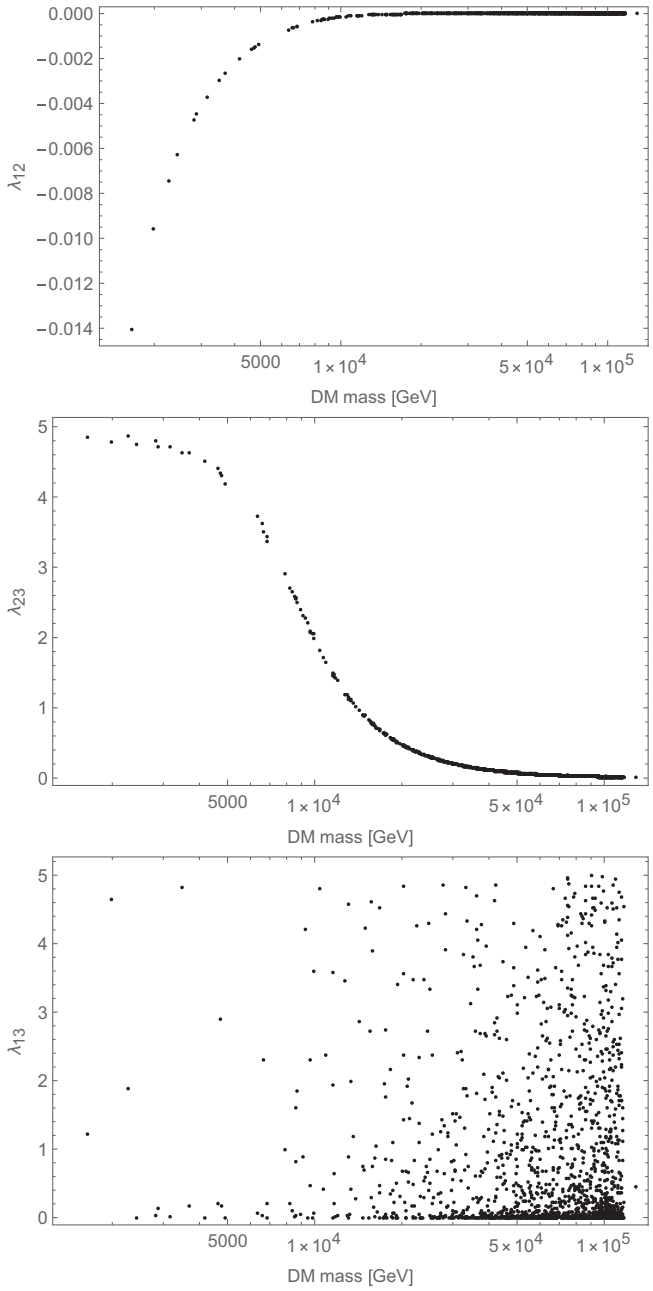

FIG. 2. Shown are the DM mass against the Higgs portal coupling λ_{12}, and the coupling λ_{13}, and λ_{23} in the model. The DM relic abundance is restricted to be the observational value $\Omega_{\rm DM}h^2 = 0.12$. Smaller DM mass requires larger Higgs portal coupling.

The thermal effective potential in the high-temperature approximation is given by [38]

$$V_{\rm eff}(T) = V + V_T = B\phi^4\left(\log\left(\frac{\phi}{\Lambda}\right) - \frac{1}{4}\right) + C\phi^2T^2 \quad (14)$$

with [39]

$$B = \frac{1}{64\pi^2}\sum_k g_k W_k^4(\theta) \quad (15a)$$

$$C = \frac{1}{12}\sum_k c_k g_k W_k^2(\theta), \quad (15b)$$

where θ is the angle which rotates (ϕ_1, ϕ_2) along the flat directions i.e., $(\phi_1 \sin\theta, \phi_2 \cos\theta)$, g_k is the number of degrees of freedom for each particle, $c_k = 1$ ($c_k = -1/2$) for bosons (fermions), and W_k is defined through $M_k(\theta, \phi) = W_k(\theta)\phi$. For the current model we have

$$W_H^2 = -2\lambda_{12} \quad (16a)$$

$$W_{\rm DM}^2 = \lambda_{13}\sin^2\theta + \lambda_{23}\cos^2\theta \quad (16b)$$

$$W_{W^\pm}^2 = \frac{1}{4}g^2\sin^2\theta \quad (16c)$$

$$W_Z^2 = \frac{1}{4}(g^2 + g'^2)\sin^2\theta \quad (16d)$$

$$W_t^2 = \frac{1}{2}y_t^2\sin^2\theta \quad (16e)$$

where $g \simeq 0.648$, $g' \simeq 0.359$ and $y_t \simeq 0.951$ are $SU(2)$ gauge coupling, $U(1)_Y$ gauge coupling, and top quark Yukawa coupling at top mass scale, respectively. The parameters B and C are

$$B = \frac{1}{64\pi^2}(W_H^4 + 6W_{W^\pm}^4 + 3W_Z^4 - 12W_t^4 + W_{\rm DM}^4) \quad (17a)$$

$$C = \frac{1}{12}(W_H^2 + 6W_{W^\pm}^2 + 3W_Z^2 + 6W_t^2 + W_{\rm DM}^2) \quad (17b)$$

The effective potential in Eq. (14) has three extrema being $\phi_{\rm min} \equiv \phi_{\rm sym} = 0$,

$$\phi_{\rm max} = \Lambda e^{\frac{1}{2}W_{-1}(-CT^2/B\Lambda^2)}, \quad (18)$$

and

$$\phi_{\rm min} \equiv \phi_{\rm brk}(T) = \Lambda e^{\frac{1}{2}W_0(-CT^2/B\Lambda^2)}, \quad (19)$$

where W_0 and W_{-1} denote respectively the principal branch and the lower real branch of the *Lambert W function*. As the argument of the W function in Eq. (19) is negative, the following condition must be held for the function to be single valued

$$-CT^2/B\Lambda^2 \geq -1/e, \quad (20)$$

that is an upper limit for temperature $T^2 \leq B\Lambda^2/Ce$, to have a nonzero VEV for the radial field ϕ. Above this

temperature limit the effective potential is in its symmetric phase with vanishing VEV.

The critical temperature is defined as the temperature at which the thermal effective potential acquires two degenerate minima, one in symmetric phase and the other in broken phase. By requiring the condition $V_{\rm eff}(v_{\rm brk}) = V_{\rm eff}(v_{\rm sym}) = 0$ we get

$$T_c = \sqrt{\frac{B}{2C}}\Lambda e^{-1/4}. \tag{21}$$

All phase transitions in scale invariant models are of first order type [19,38]. The phase transition will be strong if $v_{\rm brk}(T_c)/T_c > 1$ or equivalently

$$\sqrt{\frac{2C}{B}} > 1. \tag{22}$$

which is always true because from Eq. (17), $c > b$.

V. GRAVITATIONAL WAVES

Gravitational waves might stem from strong first-order phase transition in the early universe in different ways (see, e.g., [40]): (1) the bubble walls collisions and shocks in the plasma, $\Omega_\phi h^2$, which is the contribution of the scalar field ϕ using a technique known as "envelope approximation," (2) contributions from the sound waves, $\Omega_{\rm sw}h^2$, produced by the bubble wall collision, and (3) from the magnetohydrodynamic (MHD) turbulence in the plasma $\Omega_{\rm tur}$. The total stochastic GW background is approximately a linear combination of all contributions,

$$\Omega_{\rm GW}h^2 \simeq \Omega_\phi h^2 + \Omega_{\rm sw}h^2 + \Omega_{\rm tur} \tag{23}$$

Two key parameters are used in GW contributions; one is the ratio of the vacuum energy density released during the phase transition to the radiation energy density [41],

$$\alpha(T) = \frac{\Delta\epsilon(T)}{\rho_{\rm rad}(T)} \tag{24}$$

where

$$\rho_{\rm rad} = \pi^2 g_* T^4/30 \tag{25}$$

is the radiation energy density, and

$$\Delta\epsilon(T) = \epsilon(\phi_{\rm brk}, T) - \epsilon(\phi_{\rm sym}, T) \tag{26}$$

with

$$\epsilon(\phi, T) = -V_{\rm eff}(\phi, T) + \frac{T}{4}\frac{dV_{\rm eff}(\phi, T)}{dT} \tag{27}$$

Noting that from Eq. (14), $V_{\rm eff}(\phi_{\rm sym} = 0, T) = 0$ and $dV_{\rm eff}(\phi_{\rm sym} = 0, T)/dT = 0$, that results in $\epsilon(\phi_{\rm sym} = 0, T) = 0$, therefore we have

$$\Delta\epsilon(T) = \frac{1}{4}b\Lambda^4 e^{2W_0(-cT^2/b\Lambda^2)} \tag{28}$$

and

$$\alpha(T) = \frac{15B}{2\pi^2 g_*}\left(\frac{\Lambda}{T}\right)^4 e^{2W_0(-CT^2/B\Lambda^2)} \tag{29}$$

The other parameter is the ratio of the inverse time duration of the phase transition, β, to the Hubble parameter H_* at temperature T_*,

$$\frac{\beta}{H_*} = T\frac{d}{dT}\left(\frac{S_3(T)}{T}\right)\bigg|_{T_*}. \tag{30}$$

The temperature at which the gravitational waves are produced is denoted usually by T_*. We assume the reheating is negligible, so that the temperature at which the gravitational waves are produced is almost the nucleation temperature, i.e., $T_* \simeq T_n$. The bubble nucleation rate per unit volume is given by [42]

$$\Gamma(T) \simeq T^4\left(\frac{S_3(\phi, T)}{2\pi T}\right)^{3/2} e^{S_3(\phi,T)/T} \tag{31}$$

where $S_3(\phi, T)$ is the action for $O(3)$ symmetric bubble

$$S_3 = 4\pi\int dr r^2\left[\frac{1}{2}\left(\frac{d\phi}{dr}\right)^2 + V_{\rm eff}(\phi, T)\right]. \tag{32}$$

which is to be minimized by the ϕ (radial field) profile from $\langle\phi\rangle = 0$ to $\langle\phi\rangle \neq 0$. Here, $V_{\rm eff}(\phi, T)$ is the one-loop thermal effective potential in Eq. (14). The configuration which minimizes S_3 is the solution to

$$\frac{d^2\phi}{dr^2} + \frac{2}{r}\frac{d\phi}{dr} = \frac{dV_{\rm eff}}{d\phi}, \tag{33}$$

with boundary conditions $\phi = 0$ when $r \to \infty$ and $d\phi/dr = 0$ at $r = 0$.

For very strong electroweak phase transition the dominant contribution source of gravitational waves is due to the scalar field which is given by the envelope approximation [43–46]

$$\Omega_{\rm GW}h^2 = \left(\frac{H_*}{\beta}\right)^2\left(\frac{100}{g_*}\right)\frac{4.9\times 10^{-6}(f/f_{\rm env})^{2.8}}{1 + 2.8(f/f_{\rm env})^{3.8}} \tag{34}$$

where H_* is the Hubble parameter at the reheating temperature $T_* \simeq T_n$, $f_{\rm env}$ is the peak frequency of the spectrum in envelope approximation,

TABLE I. Shown are benchmarks for strongly first-order electroweak phase transition and gravitational wave parameters. For the four last benchmarks, the observed DM relic density cannot be fully accounted by the model due to DM dilution following the phase transition.

$M_{\rm DM}$	T_c	T_n	α	β/H_*	λ_{12}	λ_{13}	λ_{23}
346.25 GeV	114.73 GeV	65 GeV	3.28	227	-1.4×10^{-2}	1.22	4.85
1.69 TeV	911 GeV	217 GeV	103	243	-7×10^{-5}	2.37×10^{-2}	1.4
26.37 TeV	2 TeV	149 GeV	1.1×10^{4}	260	-3.08×10^{-6}	2.48×10^{-6}	0.27
36.93 TeV	2.8 TeV	117 GeV	1.1×10^{5}	252	-2.27×10^{-7}	1.32×10^{-1}	1.22×10^{-1}
81.85 TeV	6.21 TeV	47 GeV	1.08×10^{8}	1190	-3.11×10^{-8}	1.73	2.67×10^{-2}
116.64 TeV	8.86 TeV	177 GeV	2.14×10^{6}	4521	-7×10^{-9}	4.53	1.36×10^{-2}

$$\frac{f_{\rm env}}{\rm Hz} = 3.5\times10^{-6}\left(\frac{\beta}{H_*}\right)\left(\frac{g_*}{100}\right)^{1/6}\left(\frac{T_*}{100\ \rm GeV}\right) \quad (35)$$

In Table I, we have chosen from lightest to heaviest DM mass possible with corresponding parameters which give rise to the correct observed DM relic abundance. For the DM mass $m_{\rm DM}\sim 350$ GeV the coupling λ_{12} is of order 10^{-2} while for the heaviest DM mass in the table, $m_{\rm DM}\sim 100$ TeV the coupling λ_{12} becomes as small as 10^{-9}. For the parameter α that is opposite; the heavier the DM mass is, the larger parameter α becomes, i.e., from $\alpha\sim 3$ to $\alpha\sim 10^6$. For large α, due to substantial amount of latent heat and therefore a large entropy injection into the SM sector, the relic density will be diluted [47]. Taking into account this effect, the four last benchmarks in Table I, cannot account for all observed DM relic abundance. Another point in Table I is that for heavy DM there is a suppercooling in electroweak phase transitions, which is of course expected from the large values for the α parameter. Although the critical temperature lies around TeV scale, the nucleation temperature is always around the electroweak scale. For the benchmarks given in Table I we have plotted the gravitational waves signal produced during the bubble wall collisions in terms of the nucleation temperature T_n and the ratio β/H_*. The result is shown in Fig. 3. We see that the for heavy dark matter candidates in the current model, the GW signals can be detected only by AEDGE+, AEDGE and LISA with GW frequency from around 10^{-4} Hz to 0.2 Hz. This is compatible with the results in [48].

VI. CONCLUSION

We have proposed a dimensionless extension of the standard model with two extra gauge singlet scalars coupled to the standard model through a Higgs portal. In scale invariant models, the electroweak symmetry breaking occurs merely via radiation corrections a la Coleman-Weinberg. If one of the scalars does not get a nonzero VEV, it can represent the particle of dark matter. We have examined the current model when the scale of scale symmetry breaking is above TeV. At these high scales, the dark matter becomes heavy. A characteristic of this model is that even for large dark matter masses the dimensionless couplings remain very small while the direct detection constrains are evaded easily. The dark

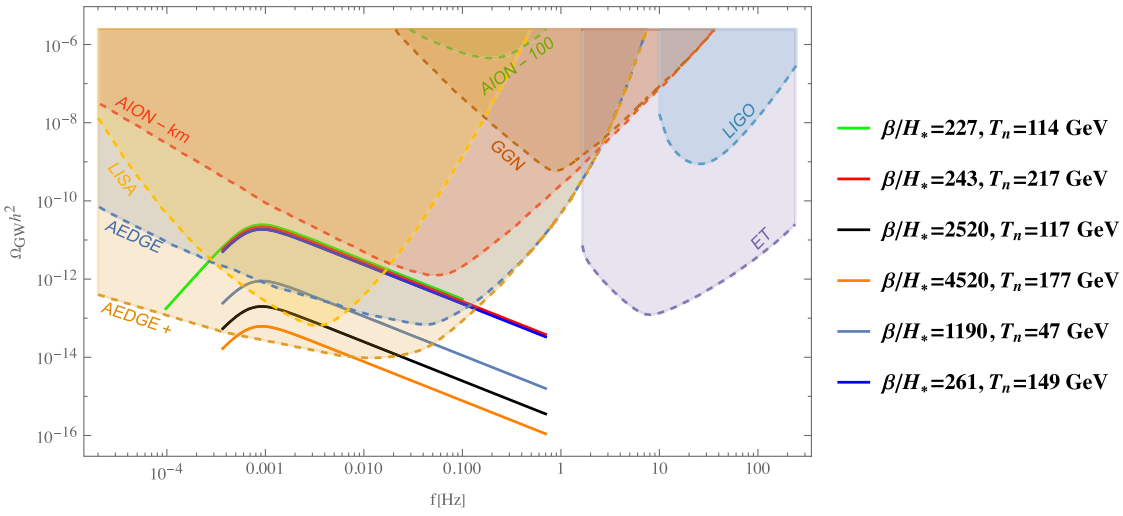

FIG. 3. Shown is the gravitational wave signals predicted from the benchmarks in Table I to be detected by space-based GW detectors.

matter mass that the model predicts is above 1.5 TeV. We have also shown analytically that the electroweak phase transition in this model is first-order and very strong. For a set of benchmarks that the relic density of dark matter is that of the observed value by WMAP and Planck, we have calculated the gravitational waves signals due to the bubble collisions during the strong electroweak phase transitions. The result is that the GW signals can be detected by future space-based gravitational wave detector AEDGE+, AEDGE and LISA in the frequency range from 10^{-4} to 0.1 Hz.

ACKNOWLEDGMENTS

I would like to acknowledge support from the International Centre for Theoretical Physics (ICTP) through the Associates Programme (2024-2029). I would also like to thank the TH department at CERN for the hospitality and support during my visit in August 2024.

[1] Georges Aad *et al.*, Observation of a new particle in the search for the Standard Model Higgs boson with the ATLAS detector at the LHC, Phys. Lett. B **716**, 1 (2012).
[2] Serguei Chatrchyan *et al.*, Observation of a new boson at a mass of 125 GeV with the CMS experiment at the LHC, Phys. Lett. B **716**, 30 (2012).
[3] Georges Aad *et al.*, Evidence for the spin-0 nature of the Higgs boson using ATLAS data, Phys. Lett. B **726**, 120 (2013).
[4] Parsa Ghorbani, Vacuum structure and electroweak phase transition in singlet scalar dark matter, Phys. Dark Universe **33**, 100861 (2021).
[5] Parsa Ghorbani, Vacuum stability vs. positivity in real singlet scalar extension of the Standard Model, Nucl. Phys. **B971**, 115533 (2021).
[6] John McDonald, Gauge singlet scalars as cold dark matter, Phys. Rev. D **50**, 3637 (1994).
[7] A. Drozd, B. Grzadkowski, and Jose Wudka, Multi-scalar-singlet extension of the Standard Model—The case for dark matter and an invisible Higgs boson, J. High Energy Phys. 04 (2012) 006; 11 (2014) 130(E).
[8] Carlos E. Yaguna, The singlet scalar as FIMP dark matter, J. High Energy Phys. 08 (2011) 060.
[9] Matthew Gonderinger, Hyungjun Lim, and Michael J. Ramsey-Musolf, Complex scalar singlet dark matter: Vacuum stability and phenomenology, Phys. Rev. D **86**, 043511 (2012).
[10] Robyn Campbell, Stephen Godfrey, Heather E. Logan, and Alexandre Poulin, Real singlet scalar dark matter extension of the Georgi-Machacek model, Phys. Rev. D **95**, 016005 (2017).
[11] Gowri Kurup and Maxim Perelstein, Dynamics of electroweak phase transition in singlet-scalar extension of the Standard Model, Phys. Rev. D **96**, 015036 (2017).
[12] Ville Vaskonen, Electroweak baryogenesis and gravitational waves from a real scalar singlet, Phys. Rev. D **95**, 123515 (2017).
[13] John Ellis, Marek Lewicki, Marco Merchand, José Miguel No, and Mateusz Zych, The scalar singlet extension of the Standard Model: Gravitational waves versus baryogenesis, J. High Energy Phys. 01 (2023) 093.
[14] Ankit Beniwal, Marek Lewicki, James D. Wells, Martin White, and Anthony G. Williams, Gravitational wave, collider and dark matter signals from a scalar singlet electroweak baryogenesis, J. High Energy Phys. 08 (2017) 108.
[15] Karim Ghorbani and Parsa Hossein Ghorbani, Strongly first-order phase transition in real singlet scalar dark matter model, J. Phys. G **47**, 015201 (2020).
[16] Karim Ghorbani and Parsa Hossein Ghorbani, A simultaneous study of dark matter and phase transition: Two-scalar scenario, J. High Energy Phys. 12 (2019) 077.
[17] Valentin V. Khoze, Inflation and dark matter in the Higgs portal of classically scale invariant Standard Model, J. High Energy Phys. 11 (2013) 215.
[18] Karim Ghorbani and Hossein Ghorbani, Scalar dark matter in scale invariant Standard Model, J. High Energy Phys. 04 (2016) 024.
[19] Parsa Hossein Ghorbani, Electroweak phase transition in the scale invariant standard model, Phys. Rev. D **98**, 115016 (2018).
[20] Seyed Yaser Ayazi and Ahmad Mohamadnejad, Scale-invariant two component dark matter, Eur. Phys. J. C **79**, 140 (2019).
[21] Basabendu Barman and Anish Ghoshal, Scale invariant FIMP miracle, J. Cosmol. Astropart. Phys. 03 (2022) 003.
[22] Amine Ahriche, Shinya Kanemura, and Masanori Tanaka, Gravitational waves from phase transitions in scale invariant models, J. High Energy Phys. 01 (2024) 201.
[23] Xiao-Rui Wong and Ke-Pan Xie, Freeze-in of WIMP dark matter, Phys. Rev. D **108**, 055035 (2023).
[24] Wei Liu and Ke-Pan Xie, Probing radiative electroweak symmetry breaking with colliders and gravitational waves, arXiv:2408.03649.
[25] Gian F. Giudice, Hyun Min Lee, Alex Pomarol, and Bibhushan Shakya, Nonthermal heavy dark matter from a first-order phase transition, arXiv:2403.03252.
[26] Eldad Gildener and Steven Weinberg, Symmetry breaking and scalar bosons, Phys. Rev. D **13**, 3333 (1976).
[27] G. Hinshaw *et al.*, Nine-year Wilkinson Microwave Anisotropy Probe (WMAP) observations: Cosmological parameter results, Astrophys. J. Suppl. Ser. **208**, 19 (2013).
[28] N. Aghanim *et al.*, Planck 2018 results. VI. Cosmological parameters, Astron. Astrophys. **641**, A6 (2020); **652**, C4(E) (2021).

[29] E. Aprile *et al.*, First dark matter search results from the XENON1T experiment, Phys. Rev. Lett. **119**, 181301 (2017).
[30] E. Aprile *et al.*, Dark matter search results from a one ton-year exposure of XENON1T, Phys. Rev. Lett. **121**, 111302 (2018).
[31] E. Aprile *et al.*, First dark matter search with nuclear recoils from the XENONnT experiment, Phys. Rev. Lett. **131**, 041003 (2023).
[32] Yue Meng *et al.*, Dark matter search results from the PandaX-4T commissioning run, Phys. Rev. Lett. **127**, 261802 (2021).
[33] J. Aalbers *et al.*, First dark matter search results from the LUX-ZEPLIN (LZ) experiment, Phys. Rev. Lett. **131**, 041002 (2023).
[34] D. S. Akerib *et al.*, Results from a search for dark matter in the complete LUX exposure, Phys. Rev. Lett. **118**, 021303 (2017).
[35] R. Ajaj *et al.*, Search for dark matter with a 231-day exposure of liquid argon using DEAP-3600 at SNOLAB, Phys. Rev. D **100**, 022004 (2019).
[36] Karim Ghorbani, Fermionic dark matter with pseudo-scalar Yukawa interaction, J. Cosmol. Astropart. Phys. 01 (2015) 015.
[37] Greg W. Anderson and Lawrence J. Hall, The electroweak phase transition and baryogenesis, Phys. Rev. D **45**, 2685 (1992).
[38] Luca Marzola, Antonio Racioppi, and Ville Vaskonen, Phase transition and gravitational wave phenomenology of scalar conformal extensions of the Standard Model, Eur. Phys. J. C **77**, 484 (2017).
[39] Francesco Sannino and Jussi Virkajärvi, First order electroweak phase transition from (non)conformal extensions of the Standard Model, Phys. Rev. D **92**, 045015 (2015).
[40] Chiara Caprini *et al.*, Science with the space-based interferometer eLISA. II: Gravitational waves from cosmological phase transitions, J. Cosmol. Astropart. Phys. 04 (2016) 001.
[41] Jose R. Espinosa, Thomas Konstandin, Jose M. No, and Geraldine Servant, Energy budget of cosmological first-order phase transitions, J. Cosmol. Astropart. Phys. 06 (2010) 028.
[42] Andrei D. Linde, Decay of the false vacuum at finite temperature, Nucl. Phys. **B216**, 421 (1983); **B223**, 544(E) (1983).
[43] Arthur Kosowsky, Michael S. Turner, and Richard Watkins, Gravitational radiation from colliding vacuum bubbles, Phys. Rev. D **45**, 4514 (1992).
[44] Arthur Kosowsky, Michael S. Turner, and Richard Watkins, Gravitational waves from first order cosmological phase transitions, Phys. Rev. Lett. **69**, 2026 (1992).
[45] Arthur Kosowsky and Michael S. Turner, Gravitational radiation from colliding vacuum bubbles: Envelope approximation to many bubble collisions, Phys. Rev. D **47**, 4372 (1993).
[46] Marc Kamionkowski, Arthur Kosowsky, and Michael S. Turner, Gravitational radiation from first order phase transitions, Phys. Rev. D **49**, 2837 (1994).
[47] Thomas Hambye, Alessandro Strumia, and Daniele Teresi, Super-cool dark matter, J. High Energy Phys. 08 (2018) 188.
[48] Valentin V. Khoze and Daniel L. Milne, Gravitational waves and dark matter from classical scale invariance, Phys. Rev. D **107**, 095012 (2023).